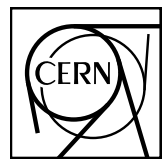


EUROPEAN ORGANIZATION FOR NUCLEAR RESEARCH



CERN-PH-EP-2012-301

10 October 2012

Measurement of the inclusive differential jet cross section in pp collisions at $\sqrt{s} = 2.76 \text{ TeV}$

The ALICE Collaboration*

Abstract

The ALICE collaboration at the CERN Large Hadron Collider reports the first measurement of the inclusive differential jet cross section at mid-rapidity in pp collisions at $\sqrt{s} = 2.76 \text{ TeV}$, based on integrated luminosity of 13.4 nb^{-1} . Calculations based on Next-to-Leading-Order perturbative QCD are in good agreement with the measurements. The measured ratio of inclusive jet cross sections for jet cone radii $R = 0.2$ and $R = 0.4$ is studied as a function of the jet transverse momentum, and is also well reproduced by a Next-to-Leading Order perturbative QCD calculation.

*See Appendix A for the list of collaboration members

1 Introduction

A QCD jet is a collimated shower of particles arising from the hadronization of a highly virtual quark or gluon generated in a hard (high momentum transfer Q^2) partonic scattering. Perturbative Quantum Chromodynamics (pQCD) calculations of inclusive jet cross sections agree with collider measurements over a wide kinematic range, for a variety of collision systems [1, 2, 3]. Jets are important tools for studying Standard Model and Beyond Standard Model physics, as well as hot and dense QCD matter that is created in high energy collisions of heavy nuclei. In heavy-ion collisions, large transverse momentum (p_T) partons traverse the colored medium and lose energy via induced gluon radiation and elastic scattering, which modify jet longitudinal and transverse structure relative to jets generated in vacuum. These modifications (“jet quenching”) are observable experimentally, and can be calculated theoretically ([4] and references therein).

Measurements of the properties of the QCD medium generated in Pb–Pb collisions at the Large Hadron Collider (LHC) require reference data from more elementary collisions (pp and pPb), where such a medium is not expected to be created. In March 2011, the LHC undertook a three-day run with pp collisions at $\sqrt{s} = 2.76$ TeV, the same center-of-mass energy as the initial Pb–Pb runs, to obtain initial measurements of such reference data. This paper reports the measurement of the inclusive differential jet cross section at mid-rapidity from that run, based on integrated luminosity of 13.4 nb^{-1} .

A QCD jet is not a uniquely defined physics observable. Jet measurements require specification of a jet reconstruction algorithm, for which there are various choices. A jet algorithm should be infrared and collinear safe, and should be applicable in a comparable way to both experimental measurements and theoretical calculations [5]. The anti- k_T algorithm [5, 6] has the required properties and is used in this analysis. A key parameter of any jet reconstruction algorithm is the “cone radius”, or resolution parameter, R , which specifies the maximum distance in pseudorapidity η and azimuthal angle φ over which the algorithm clusters constituent particles, $\sqrt{\Delta\eta^2 + \Delta\varphi^2} < R$. The inclusive jet cross section as a function of R is sensitive to the transverse structure of jets. Inclusive jet cross sections and their ratio for different values of R can be calculated using pQCD at NLO [7, 8, 9, 10]. We compare our measurements at $R = 0.2$ and $R = 0.4$ to such calculations.

2 Data Set and Detector

The data was recorded by the ALICE detector for pp collisions at $\sqrt{s} = 2.76$ TeV. ALICE detector [11] consists of two large-acceptance spectrometers: a central detector consisting of a high precision tracking system, particle identification detectors, and calorimetry, all located inside a large solenoidal magnet with field strength 0.5 T; and a forward muon spectrometer. Only the central detector is used for this analysis.

Several trigger detectors were utilized: the VZERO, consisting of segmented scintillator detectors covering the full azimuth over $2.8 < \eta < 5.1$ (VZEROA) and $-3.7 < \eta < -1.7$ (VZEROC); the SPD [12], a two-layer silicon pixel detector consisting of cylinders at radii 3.9 cm and 7.6 cm from the beam axis and covering the full azimuth over $|\eta| < 2$ and $|\eta| < 1.4$ respectively; and the EMCal [16, 17], an Electromagnetic Calorimeter covering 100 degrees in azimuth and $|\eta| < 0.7$. The EMCal consists of 10 supermodules with a total of 11520 individual towers, each covering an angular region $\Delta\eta \times \Delta\varphi = 0.014 \times 0.014$. The EMCal “Single Shower (SSh)” trigger system generates the fast sum (800 ns) of energies in overlapping groups of 4×4 adjacent EMCal towers, followed by comparison to a threshold energy. Event recording was initiated by two different trigger conditions: (i) the Minimum Bias (MB) trigger, requiring at least one hit in any of VZEROA, VZEROC, and SPD, in coincidence with the presence of a bunch crossing, and (ii) the EMCal trigger, requiring that the MB trigger condition was satisfied and that at least one SSh sum in the EMCal exceeded a nominal threshold energy of 3.0 GeV.

Events selected for offline analysis were required to have a primary vertex reconstructed within 10 cm from the center of the ALICE detector along the beam axis. After event selection cuts, the MB-triggered dataset corresponds to integrated luminosity of 0.5 nb^{-1} , while the EMCal-triggered dataset corresponds to 12.9 nb^{-1} .

For offline analysis, input to the jet reconstruction algorithm consists of charged particle tracks and EMCal clusters. Charged particle tracks are measured in the ALICE tracking system covering the full azimuth within $|\eta| < 0.9$. The tracking system consists of the ITS [12], a high precision, highly granular Inner Tracking System consisting of six silicon layers including the SPD, with inner radius 3.9 cm and outer radius 43.0 cm, and the TPC [13], a large Time Projection Chamber with inner radius 85 cm and outer radius 247 cm, that measures up to 159 independent space points per track.

Accepted tracks have a p_T -dependent minimum number of space points in the TPC, ranging from 70 at $p_T = 0.15 \text{ GeV}/c$ to 100 for $p_T > 20 \text{ GeV}/c$. In order to achieve high and azimuthally uniform tracking efficiency required for jet reconstruction, charged track selection utilizes a hybrid approach that compensates local inefficiencies in the ITS. Two distinct track classes are accepted in the hybrid approach: (i) tracks containing at least three hits in the ITS, including at least one hit in the SPD, with momentum determined without including the primary vertex (90% of all accepted tracks), and (ii) tracks containing less than three hits in the ITS or no hit in the SPD, with the primary vertex included in the momentum determination (10% of all accepted tracks). Tracks with measured $p_T > 0.15 \text{ GeV}/c$ are accepted. Tracking efficiency is $\sim 70\%$ at $p_T = 0.15 \text{ GeV}/c$, increasing with p_T to $\sim 85\%$ for $3 < p_T < 40 \text{ GeV}/c$. Charged track momentum resolution is estimated on a track-by-track basis using the covariance matrix of the Kalman track model fit [14] and by the invariant mass resolution of reconstructed Λ and K_s^0 [15]. For the first class of tracks, the resolution is $\delta p_T/p_T \sim 1\%$ at $p_T = 1.0 \text{ GeV}/c$ and $\sim 4\%$ at $p_T = 40 \text{ GeV}/c$, while for the second class of tracks the resolution is $\sim 1\%$ at $p_T = 1.0 \text{ GeV}/c$ and $\sim 8\%$ at $p_T = 40 \text{ GeV}/c$. Fake jets due to incorrect track reconstruction are identified and removed using features of the jets themselves, as described below. Charged tracks with $p_T > 40 \text{ GeV}/c$ make negligible contribution to the inclusive jet population considered in this analysis.

EMCal clusters are formed by a clustering algorithm that combines signals from adjacent EMCal towers, with cluster size limited by the requirement that each cluster contains only one local energy maximum. The systematic dependence on the clustering algorithm was explored with an alternative approach, in which clusters are strictly limited to $3 \times 3(\eta \times \phi)$ adjacent EMCal towers. This comparison results in 4% systematic uncertainty in the inclusive jet cross section (Table 1). A noise suppression threshold of 0.05 GeV is imposed on individual tower energies, and the cluster transverse energy must exceed 0.3 GeV. Noisy towers, identified by their event-averaged characteristics and comprising about 1% of all EMCal towers, are removed from the analysis. Clusters with large apparent energy but anomalously small number of contributing towers are attributed to the interaction of slow neutrons or highly ionizing particles in the avalanche photodiode of the corresponding tower, and are removed from the analysis. Charged hadrons also deposit energy in the EMCal, most commonly via minimum ionization, but also via nuclear interactions, while electrons deposit their full energy in the EMCal via an electromagnetic shower. Both charged hadron and electron contributions to EMCal cluster energy are accounted for in order to avoid double counting a fraction of their energy in the measured jet energy. Charged tracks are propagated to a depth of $10X_0$ in the EMCal [16] and matched to the closest cluster, within $\Delta\eta = 0.015$ and $\Delta\phi = 0.03$. Multiple charged hadrons can be matched to a single cluster, although the probability for this is less than 0.5% for pp collisions. Based on the measurement of negligible probability for an isolated charged track to generate an EMCal shower whose energy exceeds the track p_T [16], the energy of the matched cluster is corrected by removing 100% of the sum of all associated charged hadron momenta, and is set to zero if the remainder is negative. This procedure accurately corrects EMCal energy for clusters without contribution from photons or untracked charged particles (i.e. without “cluster pileup”). The probability for cluster pileup in pp collisions is less than 1%. The accuracy of this correc-

tion algorithm is verified by simulation, and its systematic uncertainty is estimated by varying both the fraction of the momentum sum that is subtracted and the track-cluster matching criteria.

3 Jet Reconstruction and Trigger Bias

Jet reconstruction is carried out utilizing the FastJet anti- k_T algorithm [5], with resolution parameters $R = 0.2$ and 0.4 . A jet is accepted if its centroid lies within the calorimeter acceptance, with distance at least R to the calorimeter edge. The measured cross section is corrected to acceptance $|\eta| < 0.5$ and $0 < \phi < 2\pi$.

The charged particle tracking algorithm may misidentify low p_T decay daughters from secondary vertices as primary vertex tracks and assign them a much larger p_T value. Likewise, background processes in the EMCAL can generate false neutral clusters with large apparent p_T as described above. The cuts imposed at the track or cluster level to suppress such cases directly may not be fully efficient, leading to fake jets with large apparent $p_{T,jet}$. However, such false high p_T tracks or clusters will have little additional hadronic activity in their vicinity, since they are not a part of an energetic jet. These cases are identified by examining the distribution of $z = p_{h,\text{proj}}/p_{\text{jet}}$, the magnitude of the projection of the hadron 3-momentum on the jet axis, relative to the jet momentum. Jets whose p_T is carried almost entirely by a single hadron generate a peak near $z \sim 1$ that is found to be discontinuous with the remainder of the distribution. The fake jet population due to single mis-measured tracks or clusters is therefore removed by requiring $z_{\text{leading}} < 0.98$ independent of $p_{T,jet}$, where z_{leading} refers to the z value of the most energetic hadron in the jet. The effect of the z_{leading} cut on jet reconstruction efficiency is negligible for $p_{T,jet} > 10$ GeV/c.

The jet bias imposed by the EMCAL SSh trigger must be determined, in order to extract the jet cross section from these data. Figure 1, left panel, shows the measured EMCAL cluster trigger turn-on curve from comparison of SSh-triggered clusters and clusters from MB-triggered data, for the regions of the EMCAL in which the trigger hardware was fully functional (about 90% of the acceptance). A plateau is observed for cluster energy $E > 5$ GeV. The trigger efficiency in these regions is assumed to be 100% efficient at high p_T . Due to the limited statistics of the recorded MB data set, we make an independent estimate of the jet trigger efficiency using a data-driven approach that incorporates simulation. Jet events are simulated at the detector level using the PYTHIA6 (Perugia-2011) [18] and HERWIG (version 6.510) [19] event generators, followed by detailed GEANT3 [20] transport and detector response simulation. Each simulated EMCAL cluster in the event is accepted by the trigger with probability equal to the measured cluster trigger efficiency at that energy for the supermodule in which it is located. This procedure takes into account local variations in trigger efficiencies. A simulated event is accepted by the trigger if at least one EMCAL cluster in the event satisfies the trigger requirement. The global jet trigger efficiency is determined by comparing the inclusive jet spectrum for the triggered and MB populations in the simulation. Figure 1, right panel, shows the calculated trigger efficiency for $R = 0.2$ jets (solid squares), compared to a measurement using the ratio of EMCAL-triggered and MB spectra from data (open circles). The distributions are consistent, within the precision obtained from the MB data set. The deficit at high p_T is due to the acceptance loss of the trigger system. The systematic uncertainty due to trigger efficiency arises from dependence on the hadronization model, which is assessed by comparing calculations incorporating the PYTHIA and HERWIG generators, as well as uncertainty in the online trigger threshold and in the relative scaling of SSh-triggered and MB cross sections. The resulting uncertainty increases significantly as jet p_T decreases.

The underlying event (UE) in the collision is distinct from jet fragments, and its contribution to jet transverse momentum is therefore removed for comparison to theoretical calculations. The UE energy density was estimated to be 2.1 ± 0.4 GeV/c per unit area, using dijet measurements [21] over a limited kinematic range, supplemented by PYTHIA particle-level simulations. The assigned uncertainty is estimated by the difference between data and simulations. The corresponding systematic uncertainty of the measured

cross section is 5% at $p_T = 20 \text{ GeV}/c$ and 1.5% at $p_T = 100 \text{ GeV}/c$ for $R = 0.4$ jets (see Table 1).

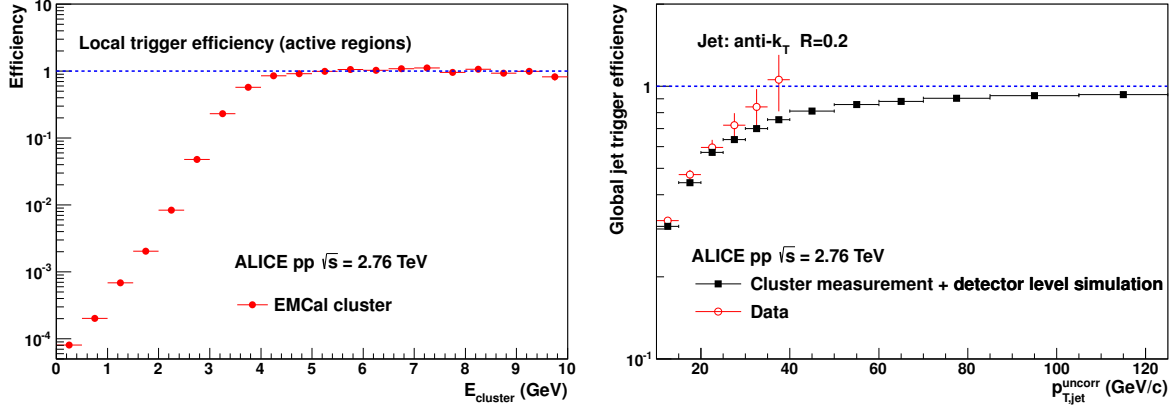


Fig. 1: Calculation of jet trigger efficiency. Left panel: EMCAL cluster trigger efficiency from data (see text) . Right panel: Global jet trigger efficiency from data (red open circles) and from PYTHIA6 detector level simulations (black solid squares), using the measured cluster efficiency from the left panel.

4 Correction to Particle Level

Jets are corrected to the particle level, without accounting for hadronization effects that may modify the energy in the jet cone at the particle level relative to the parton level [22]. This choice is made to facilitate future comparison to jet measurements in heavy-ion collisions, where correction to the parton level is difficult. A bin-by-bin technique [23], based on simulations utilizing PYTHIA6 and GEANT3, is used to correct the measured inclusive spectrum. The correction factor for a given bin is defined as

$$C_{\text{MC}}(p_T^{\text{low}}; p_T^{\text{high}}) = \frac{\int_{p_T^{\text{low}}}^{p_T^{\text{high}}} dp_T \frac{dF_{\text{meas}}^{\text{uncorr}}}{dp_T} \cdot \frac{d\sigma_{\text{MC}}^{\text{Particle}}/dp_T}{d\sigma_{\text{MC}}^{\text{Detector}}/dp_T}}{\int_{p_T^{\text{low}}}^{p_T^{\text{high}}} dp_T \frac{dF_{\text{meas}}^{\text{uncorr}}}{dp_T}}, \quad (1)$$

where $d\sigma_{\text{MC}}^{\text{Particle}}/dp_T$ is the simulated inclusive jet spectrum at the particle level from PYTHIA6; $d\sigma_{\text{MC}}^{\text{Detector}}/dp_T$ is the simulated inclusive jet spectrum at the detector level from PYTHIA6 and GEANT3, and includes all significant experimental effects; $\frac{dF_{\text{meas}}^{\text{uncorr}}}{dp_T}$ is a parametrization of the measured, uncorrected inclusive jet distribution, which provides a weight function to minimize the dependence on the spectral shape of the simulation; and p_T^{low} and p_T^{high} are the bin limits.

The detector level simulation is validated by extensive comparisons to data. An example of this comparison is given in Fig. 2, which shows the distribution of jet neutral energy fraction (NEF) for data and detector level simulation for various intervals of $p_{T,\text{jet}}$. Good agreement between data and simulation is observed. Similar levels of agreement are achieved for other key comparisons of data and simulation, including the number of charged track and EMCAL cluster constituents per jet, the z_{leading} distribution, and the mean p_T of clusters and tracks in jets.

The cumulative bin-by-bin correction factor C_{MC} arises from effects that either shift the jet energy scale (JES), or affect the shape or normalization of the inclusive spectrum. Table 1 presents the systematic uncertainty for each component of C_{MC} . Correction for unmeasured neutron and K_L^0 energy is validated by comparison of the simulation to ALICE measurements of the spectra of protons and kaons in pp collisions at $\sqrt{s} = 2.76 \text{ TeV}$ for $p_T < 20 \text{ GeV}/c$. The systematic uncertainty of C_{MC} due to this factor is estimated as the difference between PYTHIA6 and HERWIG calculations of the correction. The uncertainty in C_{MC} arising from the uncertainty in the particle-level spectrum shape is estimated by fitting the particle-level spectrum with a power law function $\sim 1/p_T^n$ ($n \sim 5$) and varying n by ± 0.5 ,

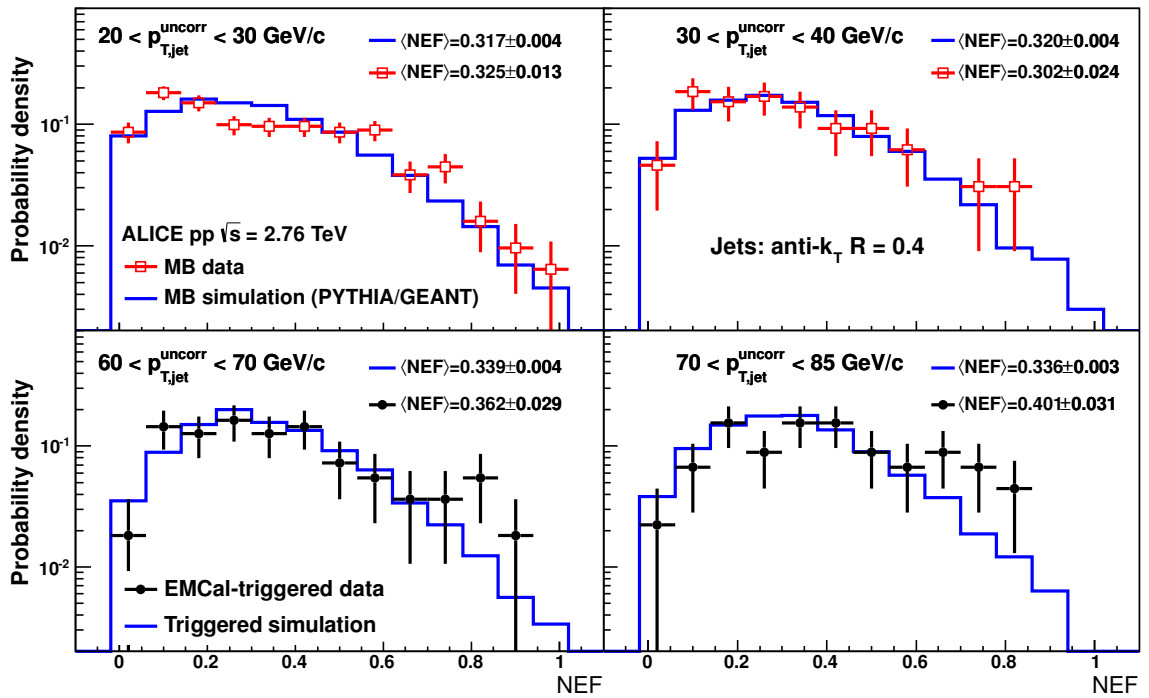


Fig. 2: Jet neutral energy fraction (NEF) distributions for minimum bias (MB) data (open squares), EMCal-triggered data (filled circles) and simulations (histograms), in four different $p_{\text{T,jet}}$ intervals (as marked).

which covers the variation in n derived from different Monte Carlo models. The main sources of the JES uncertainty are from the corrections for unmeasured neutron and K_L^0 energy and tracking efficiency. Direct contributions to the spectrum uncertainty impose smaller, but non-negligible, uncertainties to the cumulative correction factor. Uncertainties at different p_{T} are largely correlated. The components are added in quadrature to generate the cumulative uncertainty, which is labeled “Spectrum total systematic uncertainty” in Table 1, and “Systematic uncertainty” in Fig. 3 and 4.

5 Results

Figure 3 shows the inclusive differential jet cross-sections at particle level for $R = 0.2$ (left) and $R = 0.4$ (right), together with the results of pQCD calculations at NLO. In order to limit sensitivity to the systematic uncertainty of the SSh trigger efficiency, MB data are used for $p_{\text{T}} < 30$ GeV/c, whereas EMCal-triggered data are used for $p_{\text{T}} > 30$ GeV/c. The calculation shown by the green band [9] is carried out at the parton level using parton distribution functions MSTW08 [24]. The magenta band [10] represents a parton level calculation utilizing CTEQ6.6 [25], while the blue band is the same calculation including hadronization corrections [10]. The bands indicate the theoretical uncertainty estimated by varying the renormalisation and factorisation scales from 0.5 p_{T} to 2.0 p_{T} . The lower panels of Fig. 3 show the ratio of the NLO pQCD calculations to data. The calculations for both $R = 0.2$ and $R = 0.4$ are seen to agree with data within uncertainties, when hadronization effects are included.

Figure 4 shows the ratio of the measured inclusive differential jet cross sections for $R = 0.2$ and $R = 0.4$, which is sensitive to jet structure. The numerator and denominator were measured using disjoint subsets of the data, to ensure that they are statistically independent. The kinematic reach of this measurement is therefore less than that of the inclusive spectra themselves. The figure also shows parton-level pQCD calculations at Leading-Order (LO) (magenta band), NLO (orange band), and NLO with hadronization correction (blue band) [10]. This ratio allows a more stringent comparison of data and calculations

Table 1: Systematic uncertainty for each component of the corrections to the inclusive jet cross section measurement. Data at 25 GeV/c are from the MB dataset, whereas data at 100 GeV/c are from the SSh-triggered dataset. The upper section, labeled “JES uncertainty”, includes all corrections that can shift the Jet Energy Scale (JES), and the uncertainty is given as percentage of the JES. Due to the shape of the inclusive spectrum, a fractional variation in JES generates a fractional variation in cross section approximately five times larger. The lower section includes those corrections that affect the inclusive spectrum shape or normalization, with values referring to percent variation of cross section. “Spectrum total systematic uncertainty” is the cumulative uncertainty of the spectrum due to both sections of the Table, also as percent variation of cross section.

Systematic uncertainties	$R = 0.2$		$R = 0.4$	
	25 GeV/c	100 GeV/c	25 GeV/c	100 GeV/c
JES uncertainty				
Unmeasured neutron+ K_L^0	0.4%	0.7%	0.4%	0.5%
Tracking efficiency	1.4%	2.2%	1.8%	2.4%
Charged energy double-counting	0.7%	1.4%	0.6%	1.6%
Underlying event	0.2%	negligible	1.0%	0.3%
Energy scale of EMCal cluster	0.6%	0.6%	0.8%	0.8%
EMCal non-linearity	0.3%	negligible	0.6%	negligible
EMCal clustering algorithm	1.0%	1.0%	1.0%	1.0%
Momentum scale of charged tracks	negligible	negligible	negligible	negligible
Total JES uncertainty	2.0%	2.9%	2.6%	3.2%
Yield uncertainty				
Input PYTHIA spectrum shape	4%	6%	4%	7%
Dependence on fragmentation model	5%	5%	5%	5%
EMCal-SSh trigger efficiency	none	1.7%	none	1.8%
Momentum resolution of charged track	2%	2%	3%	3%
Energy resolution of EMCal cluster	1%	1%	1%	1%
Cross section normalization	1.9%	1.9%	1.9%	1.9%
Spectrum total systematic uncertainty	12.6%	17.1%	14.9%	18.4%

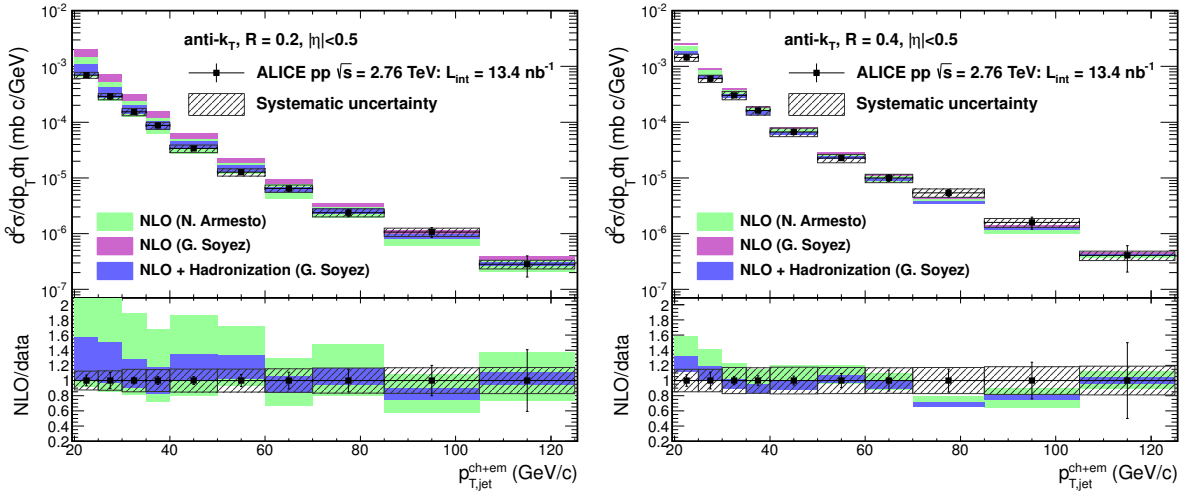


Fig. 3: Upper panels: inclusive differential jet cross section for $R = 0.2$ (left) and $R = 0.4$ (right). Vertical bars show the statistical error, while the shaded box shows the total systematic uncertainty (Table 1). The colored bands show the NLO pQCD calculations discussed in the text [9, 10]. Lower panels: ratio of NLO pQCD calculations to data. The ratio for the magenta band is not shown, for clarity.

than the individual inclusive cross sections, since systematic uncertainties that are common or highly correlated, most significantly trigger efficiency, tracking efficiency, and cross section normalization, will have smaller relative contribution to the uncertainty of the ratio. In addition, the pQCD calculation at NLO considers the ratio directly, rather than each distribution separately, and is effectively NNLO [10]. The NLO calculation with hadronization again agrees with the measurement within uncertainties.

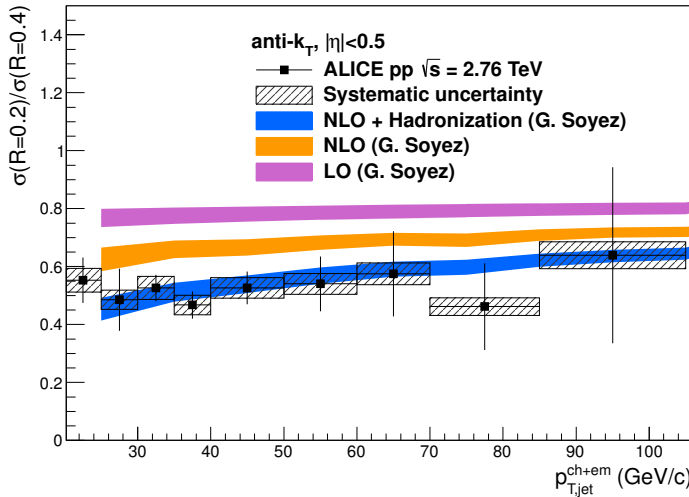


Fig. 4: Ratio of inclusive differential jet cross sections for $R = 0.2$ and $R = 0.4$, with pQCD calculations from [10].

6 Summary

In summary, we have presented the first measurement of the inclusive differential jet cross section at mid-rapidity in pp collisions at $\sqrt{s} = 2.76$ TeV. These data provide an important reference for jet measurements in heavy-ion collisions at the same $\sqrt{s_{NN}}$, as well as a test of pQCD calculations at a previously unexamined energy. NLO pQCD calculations with hadronization agree well with both inclusive jet cross section measurements at $R = 0.2$ and $R = 0.4$, and their ratio.

Acknowledgements

We congratulate the LHC for its excellent performance during the special pp run at $\sqrt{s} = 2.76$ TeV that generated these data. We thank Gregory Soyez for providing theoretical calculations.

The ALICE collaboration would like to thank all its engineers and technicians for their invaluable contributions to the construction of the experiment and the CERN accelerator teams for the outstanding performance of the LHC complex.

The ALICE collaboration acknowledges the following funding agencies for their support in building and running the ALICE detector:

Calouste Gulbenkian Foundation from Lisbon and Swiss Fonds Kidagan, Armenia;

Conselho Nacional de Desenvolvimento Científico e Tecnológico (CNPq), Financiadora de Estudos e Projetos (FINEP), Fundação de Amparo à Pesquisa do Estado de São Paulo (FAPESP);

National Natural Science Foundation of China (NSFC), the Chinese Ministry of Education (CMOE) and the Ministry of Science and Technology of China (MSTC);

Ministry of Education and Youth of the Czech Republic;

Danish Natural Science Research Council, the Carlsberg Foundation and the Danish National Research Foundation;

The European Research Council under the European Community's Seventh Framework Programme;

Helsinki Institute of Physics and the Academy of Finland;
 French CNRS-IN2P3, the ‘Region Pays de Loire’, ‘Region Alsace’, ‘Region Auvergne’ and CEA, France;
 German BMBF and the Helmholtz Association;
 General Secretariat for Research and Technology, Ministry of Development, Greece;
 Hungarian OTKA and National Office for Research and Technology (NKTH);
 Department of Atomic Energy and Department of Science and Technology of the Government of India;
 Istituto Nazionale di Fisica Nucleare (INFN) of Italy;
 MEXT Grant-in-Aid for Specially Promoted Research, Japan;
 Joint Institute for Nuclear Research, Dubna;
 National Research Foundation of Korea (NRF);
 CONACYT, DGAPA, México, ALFA-EC and the HELEN Program (High-Energy physics Latin-American–European Network);
 Stichting voor Fundamenteel Onderzoek der Materie (FOM) and the Nederlandse Organisatie voor Wetenschappelijk Onderzoek (NWO), Netherlands;
 Research Council of Norway (NFR);
 Polish Ministry of Science and Higher Education;
 National Authority for Scientific Research - NASR (Autoritatea Națională pentru Cercetare Științifică - ANCS);
 Federal Agency of Science of the Ministry of Education and Science of Russian Federation, International Science and Technology Center, Russian Academy of Sciences, Russian Federal Agency of Atomic Energy, Russian Federal Agency for Science and Innovations and CERN-INTAS;
 Ministry of Education of Slovakia;
 Department of Science and Technology, South Africa;
 CIEMAT, EELA, Ministerio de Educación y Ciencia of Spain, Xunta de Galicia (Consellería de Educación), CEADEN, Cubaenergía, Cuba, and IAEA (International Atomic Energy Agency);
 Swedish Research Council (VR) and Knut & Alice Wallenberg Foundation (KAW);
 Ukraine Ministry of Education and Science;
 United Kingdom Science and Technology Facilities Council (STFC);
 The United States Department of Energy, the United States National Science Foundation, the State of Texas, and the State of Ohio.

References

- [1] G. Aad *et al.* [ATLAS Collaboration], Eur. Phys. J. C **71**, 1512 (2011) [arXiv:1009.5908v2].
- [2] S. Chatrchyan *et al.* [CMS Collaboration], Phys. Rev. Lett. **107**, 132001 (2011).
- [3] T. Affolder *et al.* [CDF Collaboration], Phys. Rev. D **64**, 032001 (2001).
- [4] A. Majumder and M. Van Leeuwen, Prog. Part. Nucl. Phys. A **66**, 41-92 (2011) [arXiv:1002.2206].
- [5] M. Cacciari, G. P. Salam and G. Soyez, JHEP **04**, 063 (2008) [arXiv:0802.1189].
- [6] M. Cacciari, G. P. Salam and G. Soyez, Eur. Phys. J. C **72**, 1896 (2012) [arXiv:1111.6097].
- [7] S. Frixione, Z. Kunszt, and A. Signer, Nucl. Phys. B **467**, 399-442 (1996).
- [8] S. Frixione, Nucl. Phys. B **507**, 295-314 (1997)
- [9] N. Armesto, private communication. Calculations based on [7, 8].
- [10] G. Soyez, Phys. Lett. B **698**, 59 (2011) [arXiv:1101.2665v1]; private communication.
- [11] K. Aamodt *et al.* [ALICE Collaboration], JINST **3**, S08002 (2008) [arXiv:1001.0502v3].
- [12] K. Aamodt *et al.* [ALICE Collaboration], JINST **5**, P03003 (2010).
- [13] J. Alme *et al.* [ALICE Collaboration], Nucl. Instr. Meth. A **622**, 316 (2010).
- [14] R. Fröhwirth, Nucl. Instr. Meth. A **262**, 444 (1987).

- [15] B. Abelev *et al.* [ALICE Collaboration], [arXiv:1208.2711].
- [16] P. Cortese *et al.* [ALICE EMCal Collaboration], CERN-ALICE-TDR-014 (2008).
- [17] J. Allen *et al.* [ALICE EMCAL Collaboration], Nucl. Instr. Meth. A **615**, 6-13 (2010) [arXiv:0912.2005].
- [18] T. Sjostrand *et al.*, JHEP **05**, 026 (2006) [arXiv:0603175v2].
- [19] G. Corcella *et al.*, JHEP **0101**, 010 (2001) [arXiv: 0011363v3].
- [20] R. Brun, F. Bruyant, M. Maire, A. C. McPherson and P. Zanarini, CERN Data Handling Division DD/EE/84-1 (1985).
- [21] CDF note CDF/ANAL/CDF/CDFR/7703.
- [22] A. Bhatti *et al.* [CDF Collaboration], Nucl. Instr. Meth. A **566**, 375 (2006).
- [23] G. Cowan, Proc. Advanced Statistical Techniques in Particle Physics (2002).
- [24] A. D. Martin, W. J. Stirling, R. S. Thorne and G. Watt, Eur. Phys. J. C **63**, 189-285 (2009) [arXiv:0901.0002].
- [25] P. M. Nadolsky, H. Lai, Q. Cao, J. Huston and J. Pumplin *et al.*, Phys. Rev. D **78**, 013004 (2008) [arXiv:0802.0007].

A The ALICE Collaboration

B. Abelev⁷¹, J. Adam³⁶, D. Adamová⁷⁷, A.M. Adare¹²³, M.M. Aggarwal⁸¹, G. Aglieri Rinella³², M. Agnello¹⁰¹, A.G. Agocs⁶³, A. Agostinelli²², Z. Ahammed¹¹⁹, A. Ahmad Masoodi¹⁶, N. Ahmad¹⁶, S.U. Ahn^{39,65}, S.A. Ahn⁶⁵, M. Ajaz¹⁴, A. Akindinov⁴⁹, D. Aleksandrov⁹², B. Alessandro¹⁰¹, R. Alfaro Molina⁵⁹, A. Alici^{103,11}, A. Alkin², E. Almaráz Aviña⁵⁹, J. Alme³⁴, T. Alt³⁸, V. Altini³⁰, S. Altinpinar¹⁷, I. Altsybeev¹²⁰, C. Andrei⁷⁴, A. Andronic⁸⁹, V. Anguelov⁸⁶, J. Anielski⁵⁷, C. Anson¹⁸, T. Antičić⁹⁰, F. Antinori⁹⁷, P. Antonioli¹⁰³, L. Aphecetche¹⁰⁵, H. Appelshäuser⁵⁵, N. Arbor⁶⁷, S. Arcelli²², A. Arend⁵⁵, N. Armesto¹⁵, R. Arnaldi¹⁰¹, T. Aronsson¹²³, I.C. Arsene⁸⁹, M. Arslandok⁵⁵, A. Asryan¹²⁰, A. Augustinus³², R. Averbeck⁸⁹, T.C. Awes⁷⁸, J. Äystö⁴¹, M.D. Azmi^{16,83}, M. Bach³⁸, A. Badalà⁹⁹, Y.W. Baek^{66,39}, R. Bailhache⁵⁵, R. Bala¹⁰¹, R. Baldini Ferroli¹¹, A. Baldissari¹³, F. Baltasar Dos Santos Pedrosa³², J. Bán⁵⁰, R.C. Baral⁵¹, R. Barbera²⁶, F. Barile³⁰, G.G. Barnaföldi⁶³, L.S. Barnby⁹⁴, V. Barret⁶⁶, J. Bartke¹⁰⁷, M. Basile²², N. Bastid⁶⁶, S. Basu¹¹⁹, B. Bathen⁵⁷, G. Batigne¹⁰⁵, B. Batyunya⁶², C. Baumann⁵⁵, I.G. Bearden⁷⁵, H. Beck⁵⁵, N.K. Behera⁴³, I. Belikov⁶¹, F. Bellini²², R. Bellwied¹¹³, E. Belmont-Moreno⁵⁹, G. Bencedi⁶³, S. Beole²⁴, I. Berceanu⁷⁴, A. Bercuci⁷⁴, Y. Berdnikov⁷⁹, D. Berenyi⁶³, A.A.E. Bergognon¹⁰⁵, D. Berzano¹⁰¹, L. Betev³², A. Bhasin⁸⁴, A.K. Bhati⁸¹, J. Bhom¹¹⁷, N. Bianchi⁶⁸, L. Bianchi²⁴, C. Bianchin²⁷, J. Bielčík³⁶, J. Bielčíková⁷⁷, A. Bilandzic⁷⁵, S. Bjelogrlic⁴⁸, F. Blanco¹¹³, F. Blanco⁹, D. Blau⁹², C. Blume⁵⁵, M. Boccioli³², N. Bock¹⁸, S. Böttger⁵⁴, A. Bogdanov⁷², H. Bøggild⁷⁵, M. Bogolyubsky⁴⁶, L. Boldizsár⁶³, M. Bombara³⁷, J. Book⁵⁵, H. Borel¹³, A. Borissov¹²², F. Bossú⁸³, M. Botje⁷⁶, E. Botta²⁴, B. Boyer⁴⁵, E. Braidot⁷⁰, P. Braun-Munzinger⁸⁹, M. Bregant¹⁰⁵, T. Breitner⁵⁴, T.A. Browning⁸⁷, M. Broz³⁵, R. Brun³², E. Bruna^{24,101}, G.E. Bruno³⁰, D. Budnikov⁹¹, H. Buesching⁵⁵, S. Bufalino^{24,101}, O. Busch⁸⁶, Z. Buthelezi⁸³, D. Caballero Orduna¹²³, D. Caffarri^{27,97}, X. Cai⁶, H. Caines¹²³, E. Calvo Villar⁹⁵, P. Camerini²³, V. Canoa Roman¹⁰, G. Cara Romeo¹⁰³, F. Carena³², W. Carena³², N. Carlin Filho¹¹⁰, F. Carminati³², A. Casanova Díaz⁶⁸, J. Castillo Castellanos¹³, J.F. Castillo Hernandez⁸⁹, E.A.R. Casula²¹, V. Catanescu⁷⁴, C. Cavicchioli³², C. Ceballos Sanchez⁸, J. Cepila³⁶, P. Cerello¹⁰¹, B. Chang^{41,126}, S. Chapelard³², J.L. Charvet¹³, S. Chattopadhyay¹¹⁹, S. Chattopadhyay⁹³, I. Chawla⁸¹, M. Cherney⁸⁰, C. Cheshkov^{32,112}, B. Cheynis¹¹², V. Chibante Barroso³², D.D. Chinellato¹¹³, P. Chochula³², M. Chojnacki^{75,48}, S. Choudhury¹¹⁹, P. Christakoglou⁷⁶, C.H. Christensen⁷⁵, P. Christiansen³¹, T. Chujo¹¹⁷, S.U. Chung⁸⁸, C. Cicalo¹⁰⁰, L. Cifarelli^{22,32,11}, F. Cindolo¹⁰³, J. Cleymans⁸³, F. Coccetti¹¹, F. Colamaria³⁰, D. Colella³⁰, A. Collu²¹, G. Conesa Balbastre⁶⁷, Z. Conesa del Valle³², G. Contin²³, J.G. Contreras¹⁰, T.M. Cormier¹²², Y. Corrales Morales²⁴, P. Cortese²⁹, I. Cortés Maldonado¹, M.R. Cosentino⁷⁰, F. Costa³², M.E. Cotallo⁹, E. Crescio¹⁰, P. Crochet⁶⁶, E. Cruz Alaniz⁵⁹, E. Cuautle⁵⁸, L. Cunqueiro⁶⁸, A. Dainese^{27,97}, H.H. Dalsgaard⁷⁵, A. Danu⁵³, I. Das⁴⁵, D. Das⁹³, S. Das³, K. Das⁹³, S. Dash⁴³, A. Dash¹¹¹, S. De¹¹⁹, G.O.V. de Barros¹¹⁰, A. De Caro^{28,11}, G. de Cataldo⁹⁶, J. de Cuveland³⁸, A. De Falco²¹, D. De Gruttola²⁸, H. Delagrange¹⁰⁵, A. Deloff⁷³, N. De Marco¹⁰¹, E. Dénes⁶³, S. De Pasquale²⁸, A. Deppman¹¹⁰, G. D Erasmo³⁰, R. de Rooij⁴⁸, M.A. Diaz Corchero⁹, D. Di Bari³⁰, T. Dietel⁵⁷, C. Di Giglio³⁰, S. Di Liberto⁹⁸, A. Di Mauro³², P. Di Nezza⁶⁸, R. Divia³², Ø. Djupsland¹⁷, A. Dobrin^{122,31}, T. Dobrowolski⁷³, I. Domínguez⁵⁸, B. Dönigus⁸⁹, O. Dordic²⁰, O. Driga¹⁰⁵, A.K. Dubey¹¹⁹, A. Dubla⁴⁸, L. Ducroux¹¹², P. Dupieux⁶⁶, A.K. Dutta Majumdar⁹³, M.R. Dutta Majumdar¹¹⁹, D. Elia⁹⁶, D. Emschermann⁵⁷, H. Engel⁵⁴, B. Erazmus^{32,105}, H.A. Erdal³⁴, B. Espagnon⁴⁵, M. Estienne¹⁰⁵, S. Esumi¹¹⁷, D. Evans⁹⁴, G. Eyyubova²⁰, D. Fabris^{27,97}, J. Faivre⁶⁷, D. Falchieri²², A. Fantoni⁶⁸, M. Fasel⁸⁹, R. Fearick¹⁷, L. Feldkamp⁵⁷, D. Felea⁵³, A. Feliciello¹⁰¹, B. Fenton-Olsen⁷⁰, G. Feofilov¹²⁰, A. Fernández Téllez¹, R. Ferretti²⁹, A. Ferretti²⁴, A. Festanti²⁷, J. Figiel¹⁰⁷, M.A.S. Figueredo¹¹⁰, S. Filchagin⁹¹, D. Finogeev⁴⁷, F.M. Fionda³⁰, E.M. Fiore³⁰, M. Floris³², S. Foertsch⁸³, P. Foka⁸⁹, S. Fokin⁹², E. Fragiacomo¹⁰², A. Francescon^{32,27}, U. Frankenfeld⁸⁹, U. Fuchs³², C. Furget⁶⁷, M. Fusco Girard²⁸, J.J. Gaardhøje⁷⁵, M. Gagliardi²⁴, A. Gago⁹⁵, M. Gallio²⁴, D.R. Gangadharan¹⁸, P. Ganoti⁷⁸, C. Garabatos⁸⁹, E. Garcia-Solis¹², I. Garishvili⁷¹, J. Gerhard³⁸, M. Germain¹⁰⁵, C. Geuna¹³, M. Gheata^{53,32}, A. Gheata³², P. Ghosh¹¹⁹, P. Gianotti⁶⁸, M.R. Girard¹²¹, P. Giubellino³², E. Gladysz-Dziadus¹⁰⁷, P. Glässel⁸⁶, R. Gomez^{109,10}, E.G. Ferreiro¹⁵, L.H. González-Trueba⁵⁹, P. González-Zamora⁹, S. Gorbunov³⁸, A. Goswami⁸⁵, S. Gotovac¹⁰⁶, V. Grabski⁵⁹, L.K. Graczykowski¹²¹, R. Grajcarek⁸⁶, A. Grelli⁴⁸, C. Grigoras³², A. Grigoras³², V. Grigoriev⁷², A. Grigoryan¹²⁴, S. Grigoryan⁶², B. Grinyov², N. Grion¹⁰², P. Gros³¹, J.F. Grosse-Oetringhaus³², J.-Y. Grossiord¹¹², R. Grossi³², F. Guber⁴⁷, R. Guernane⁶⁷, C. Guerra Gutierrez⁹⁵, B. Guerzoni²², M. Guilbaud¹¹², K. Gulbrandsen⁷⁵, H. Gulkanyan¹²⁴, T. Gunji¹¹⁶, A. Gupta⁸⁴, R. Gupta⁸⁴, Ø. Haaland¹⁷, C. Hadjidakis⁴⁵, M. Haiduc⁵³, H. Hamagaki¹¹⁶, G. Hamar⁶³, B.H. Han¹⁹, L.D. Hanratty⁹⁴, A. Hansen⁷⁵, Z. Harmanová-Tóthová³⁷, J.W. Harris¹²³, M. Hartig⁵⁵, A. Harton¹², D. Hasegan⁵³, D. Hatzifotiadou¹⁰³, A. Hayrapetyan^{32,124}, S.T. Heckel⁵⁵, M. Heide⁵⁷, H. Helstrup³⁴, A. Herghhelegiu⁷⁴, G. Herrera Corral¹⁰,

- N. Herrmann⁸⁶, B.A. Hess¹¹⁸, K.F. Hetland³⁴, B. Hicks¹²³, B. Hippolyte⁶¹, Y. Hori¹¹⁶, P. Hristov³², I. Hřivnáčová⁴⁵, M. Huang¹⁷, T.J. Humanic¹⁸, D.S. Hwang¹⁹, R. Ichou⁶⁶, R. Ilkaev⁹¹, I. Ilkiv⁷³, M. Inaba¹¹⁷, E. Incani²¹, P.G. Innocenti³², G.M. Innocenti²⁴, M. Ippolitov⁹², M. Irfan¹⁶, C. Ivan⁸⁹, A. Ivanov¹²⁰, V. Ivanov⁷⁹, M. Ivanov⁸⁹, O. Ivanytskyi², A. Jacholkowski²⁶, P. M. Jacobs⁷⁰, H.J. Jang⁶⁵, R. Janik³⁵, M.A. Janik¹²¹, P.H.S.Y. Jayarathna¹¹³, S. Jena⁴³, D.M. Jha¹²², R.T. Jimenez Bustamante⁵⁸, P.G. Jones⁹⁴, H. Jung³⁹, A. Jusko⁹⁴, A.B. Kaidalov⁴⁹, S. Kalcher³⁸, P. Kaliňák⁵⁰, T. Kalliokoski⁴¹, A. Kalweit^{56,32}, J.H. Kang¹²⁶, V. Kaplin⁷², A. Karasu Uysal^{32,125}, O. Karavichev⁴⁷, T. Karavicheva⁴⁷, E. Karpechev⁴⁷, A. Kazantsev⁹², U. Kebschull⁵⁴, R. Keidel¹²⁷, M.M. Khan¹⁶, S.A. Khan¹¹⁹, P. Khan⁹³, K. H. Khan¹⁴, A. Khanzadeev⁷⁹, Y. Kharlov⁴⁶, B. Kileng³⁴, M. Kim¹²⁶, D.W. Kim^{39,65}, J.H. Kim¹⁹, J.S. Kim³⁹, M. Kim³⁹, D.J. Kim⁴¹, S. Kim¹⁹, T. Kim¹²⁶, B. Kim¹²⁶, S. Kirsch³⁸, I. Kisiel³⁸, S. Kiselev⁴⁹, A. Kisiel¹²¹, J.L. Klay⁵, J. Klein⁸⁶, C. Klein-Bösing⁵⁷, M. Kliemant⁵⁵, A. Kluge³², M.L. Knichel⁸⁹, A.G. Knospe¹⁰⁸, K. Koch⁸⁶, M.K. Köhler⁸⁹, T. Kollegger³⁸, A. Kolojvari¹²⁰, V. Kondratiev¹²⁰, N. Kondratyeva⁷², A. Konevskikh⁴⁷, R. Kour⁹⁴, M. Kowalski¹⁰⁷, S. Kox⁶⁷, G. Koyithatta Meethaleveedu⁴³, J. Kral⁴¹, I. Králik⁵⁰, F. Kramer⁵⁵, A. Kravčáková³⁷, T. Krawutschke^{86,33}, M. Krelina³⁶, M. Kretz³⁸, M. Krivda^{94,50}, F. Krizek⁴¹, M. Krus³⁶, E. Kryshen⁷⁹, M. Krzewicki⁸⁹, Y. Kucheriaev⁹², T. Kugathasan³², C. Kuhn⁶¹, P.G. Kuijer⁷⁶, I. Kulakov⁵⁵, J. Kumar⁴³, P. Kurashvili⁷³, A. Kurepin⁴⁷, A.B. Kurepin⁴⁷, A. Kuryakin⁹¹, S. Kushpil⁷⁷, V. Kushpil⁷⁷, H. Kvaerno²⁰, M.J. Kweon⁸⁶, Y. Kwon¹²⁶, P. Ladrón de Guevara⁵⁸, I. Lakomov⁴⁵, R. Langoy¹⁷, S.L. La Pointe⁴⁸, C. Lara⁵⁴, A. Lardeux¹⁰⁵, P. La Rocca²⁶, R. Lea²³, M. Lechman³², G.R. Lee⁹⁴, K.S. Lee³⁹, S.C. Lee³⁹, J. Lehnert⁵⁵, M. Lenhardt⁸⁹, V. Lenti⁹⁶, H. León⁵⁹, M. Leoncino¹⁰¹, I. León Monzón¹⁰⁹, H. León Vargas⁵⁵, P. Lévai⁶³, J. Lien¹⁷, R. Lietava⁹⁴, S. Lindal²⁰, V. Lindenstruth³⁸, C. Lippmann^{89,32}, M.A. Lisa¹⁸, H.M. Ljunggren³¹, P.I. Loenne¹⁷, V.R. Loggins¹²², V. Loginov⁷², S. Lohn³², D. Lohner⁸⁶, C. Loizides⁷⁰, K.K. Loo⁴¹, X. Lopez⁶⁶, E. López Torres⁸, G. Løvhøiden²⁰, X.-G. Lu⁸⁶, P. Luettig⁵⁵, M. Lunardon²⁷, J. Luo⁶, G. Luparello⁴⁸, C. Luzzi³², R. Ma¹²³, K. Ma⁶, D.M. Madagodahettige-Don¹¹³, A. Maevskaya⁴⁷, M. Mager^{56,32}, D.P. Mahapatra⁵¹, A. Maire⁸⁶, M. Malaev⁷⁹, I. Maldonado Cervantes⁵⁸, L. Malinina^{62,ii}, D. Mal'Kevich⁴⁹, P. Malzacher⁸⁹, A. Mamontov⁹¹, L. Manceau¹⁰¹, L. Mangotra⁸⁴, V. Manko⁹², F. Manso⁶⁶, V. Manzari⁹⁶, Y. Mao⁶, M. Marchisone^{66,24}, J. Mareš⁵², G.V. Margagliotti^{23,102}, A. Margotti¹⁰³, A. Marín⁸⁹, C.A. Marin Tobon³², C. Markert¹⁰⁸, M. Marquard⁵⁵, I. Martashvili¹¹⁵, N.A. Martin⁸⁹, P. Martinengo³², M.I. Martínez¹, A. Martínez Davalos⁵⁹, G. Martínez García¹⁰⁵, Y. Martynov², A. Mas¹⁰⁵, S. Masciocchi⁸⁹, M. Masera²⁴, A. Masoni¹⁰⁰, L. Massacrier¹⁰⁵, A. Mastroserio³⁰, Z.L. Matthews⁹⁴, A. Matyja^{107,105}, C. Mayer¹⁰⁷, J. Mazer¹¹⁵, M.A. Mazzoni⁹⁸, F. Meddi²⁵, A. Menchaca-Rocha⁵⁹, J. Mercado Pérez⁸⁶, M. Meres³⁵, Y. Miake¹¹⁷, L. Milano²⁴, J. Milosevic^{20,iii}, A. Mischke⁴⁸, A.N. Mishra⁸⁵, D. Miškowiec^{89,32}, C. Mitu⁵³, S. Mizuno¹¹⁷, J. Mlynarz¹²², B. Mohanty¹¹⁹, L. Molnar^{63,32,61}, L. Montaño Zetina¹⁰, M. Monteno¹⁰¹, E. Montes⁹, T. Moon¹²⁶, M. Morando²⁷, D.A. Moreira De Godoy¹¹⁰, S. Moretto²⁷, A. Morsch³², V. Muccifora⁶⁸, E. Mudnic¹⁰⁶, S. Muhuri¹¹⁹, M. Mukherjee¹¹⁹, H. Müller³², M.G. Munhoz¹¹⁰, L. Musa³², A. Musso¹⁰¹, B.K. Nandi⁴³, R. Nania¹⁰³, E. Nappi⁹⁶, C. Nattrass¹¹⁵, S. Navin⁹⁴, T.K. Nayak¹¹⁹, S. Nazarenko⁹¹, A. Nedosekin⁴⁹, M. Nicassio^{30,89}, M. Niculescu^{53,32}, B.S. Nielsen⁷⁵, T. Niida¹¹⁷, S. Nikolaev⁹², V. Nikolic⁹⁰, S. Nikulin⁹², V. Nikulin⁷⁹, B.S. Nilsen⁸⁰, M.S. Nilsson²⁰, F. Noferini^{103,11}, P. Nomokonov⁶², G. Nooren⁴⁸, N. Novitzky⁴¹, A. Nyanin⁹², A. Nyatha⁴³, C. Nygaard⁷⁵, J. Nystrand¹⁷, A. Ochirov¹²⁰, H. Oeschler^{56,32}, S. Oh¹²³, S.K. Oh³⁹, J. Oleniacz¹²¹, A.C. Oliveira Da Silva¹¹⁰, C. Oppedisano¹⁰¹, A. Ortiz Velasquez^{31,58}, A. Oskarsson³¹, P. Ostrowski¹²¹, J. Otwinowski⁸⁹, K. Oyama⁸⁶, K. Ozawa¹¹⁶, Y. Pachmayer⁸⁶, M. Pachr³⁶, F. Padilla²⁴, P. Pagano²⁸, G. Paić⁵⁸, F. Painke³⁸, C. Pajares¹⁵, S.K. Pal¹¹⁹, A. Palaha⁹⁴, A. Palmeri⁹⁹, V. Papikyan¹²⁴, G.S. Pappalardo⁹⁹, W.J. Park⁸⁹, A. Passfeld⁵⁷, B. Pastirčák⁵⁰, D.I. Patalakha⁴⁶, V. Paticchio⁹⁶, B. Paul⁹³, A. Pavlinov¹²², T. Pawlak¹²¹, T. Peitzmann⁴⁸, H. Pereira Da Costa¹³, E. Pereira De Oliveira Filho¹¹⁰, D. Peresunko⁹², C.E. Pérez Lara⁷⁶, E. Perez Lezama⁵⁸, D. Perini³², D. Perrino³⁰, W. Peryt¹²¹, A. Pesci¹⁰³, V. Peskov^{32,58}, Y. Pestov⁴, V. Petráček³⁶, M. Petran³⁶, M. Petris⁷⁴, P. Petrov⁹⁴, M. Petrovici⁷⁴, C. Petta²⁶, S. Piano¹⁰², A. Piccotti¹⁰¹, M. Píkna³⁵, P. Pillot¹⁰⁵, O. Pinazza³², L. Pinsky¹¹³, N. Pitz⁵⁵, D.B. Piyarathna¹¹³, M. Planinic⁹⁰, M. Płoskoń⁷⁰, J. Pluta¹²¹, T. Pocheptsov⁶², S. Pochybova⁶³, P.L.M. Podesta-Lerma¹⁰⁹, M.G. Poghosyan^{32,24}, K. Polák⁵², B. Polichtchouk⁴⁶, A. Pop⁷⁴, S. Porteboeuf-Houssais⁶⁶, V. Pospíšil³⁶, B. Potukuchi⁸⁴, S.K. Prasad¹²², R. Preghenella^{103,11}, F. Prino¹⁰¹, C.A. Pruneau¹²², I. Pschenichnov⁴⁷, G. Puddu²¹, A. Pulvirenti²⁶, V. Punin⁹¹, M. Putiš³⁷, J. Putschke¹²², E. Quercigh³², H. Qvigstad²⁰, A. Rachevski¹⁰², A. Rademakers³², T.S. Räihä⁴¹, J. Rak⁴¹, A. Rakotozafindrabe¹³, L. Ramello²⁹, A. Ramírez Reyes¹⁰, S. Raniwala⁸⁵, R. Raniwala⁸⁵, S.S. Räsänen⁴¹, B.T. Rascanu⁵⁵, D. Rathee⁸¹, K.F. Read¹¹⁵, J.S. Real⁶⁷, K. Redlich^{73,60}, R.J. Reed¹²³, A. Rehman¹⁷, P. Reichelt⁵⁵, M. Reicher⁴⁸, R. Renfordt⁵⁵, A.R. Reolon⁶⁸, A. Reshetin⁴⁷, F. Rettig³⁸, J.-P. Revol³², K. Reygers⁸⁶, L. Riccati¹⁰¹, R.A. Ricci⁶⁹, T. Richert³¹, M. Richter²⁰, P. Riedler³², W. Riegler³², F. Rigg^{26,99}, M. Rodríguez Cahuantzi¹,

A. Rodriguez Manso⁷⁶, K. Røed^{17,20}, D. Rohr³⁸, D. Röhrich¹⁷, R. Romita⁸⁹, F. Ronchetti⁶⁸, P. Rosnet⁶⁶, S. Rossegger³², A. Rossi^{32,27}, P. Roy⁹³, C. Roy⁶¹, A.J. Rubio Montero⁹, R. Rui²³, R. Russo²⁴, E. Ryabinkin⁹², A. Rybicki¹⁰⁷, S. Sadovsky⁴⁶, K. Šafařík³², R. Sahoo⁴⁴, P.K. Sahu⁵¹, J. Saini¹¹⁹, H. Sakaguchi⁴², S. Sakai⁷⁰, D. Sakata¹¹⁷, C.A. Salgado¹⁵, J. Salzwedel¹⁸, S. Sambyal⁸⁴, V. Samsonov⁷⁹, X. Sanchez Castro⁶¹, L. Šádor⁵⁰, A. Sandoval⁵⁹, S. Sano¹¹⁶, M. Sano¹¹⁷, R. Santoro^{32,11}, J. Sarkamo⁴¹, E. Scapparone¹⁰³, F. Scarlassara²⁷, R.P. Scharenberg⁸⁷, C. Schiaua⁷⁴, R. Schicker⁸⁶, C. Schmidt⁸⁹, H.R. Schmidt¹¹⁸, S. Schreiner³², S. Schuchmann⁵⁵, J. Schukraft³², T. Schuster¹²³, Y. Schutz^{32,105}, K. Schwarz⁸⁹, K. Schweda⁸⁹, G. Scioli²², E. Scomparin¹⁰¹, R. Scott¹¹⁵, P.A. Scott⁹⁴, G. Segato²⁷, I. Selyuzhenkov⁸⁹, S. Senyukov⁶¹, J. Seo⁸⁸, S. Serici²¹, E. Serradilla^{9,59}, A. Sevcenco⁵³, A. Shabetai¹⁰⁵, G. Shabratova⁶², R. Shahoyan³², S. Sharma⁸⁴, N. Sharma^{81,115}, S. Rohni⁸⁴, K. Shigaki⁴², K. Shtejer⁸, Y. Sibiriak⁹², M. Siciliano²⁴, E. Sickling³², S. Siddhanta¹⁰⁰, T. Siemiaczuk⁷³, D. Silvermyr⁷⁸, C. Silvestre⁶⁷, G. Simatovic^{58,90}, G. Simonetti³², R. Singaraju¹¹⁹, R. Singh⁸⁴, S. Singha¹¹⁹, V. Singhal¹¹⁹, B.C. Sinha¹¹⁹, T. Sinha⁹³, B. Sitar³⁵, M. Sitta²⁹, T.B. Skaali²⁰, K. Skjerdal¹⁷, R. Smakal³⁶, N. Smirnov¹²³, R.J.M. Snellings⁴⁸, C. Søgaard^{75,31}, R. Soltz⁷¹, H. Son¹⁹, M. Song¹²⁶, J. Song⁸⁸, C. Soos³², F. Soramel²⁷, I. Sputowska¹⁰⁷, M. Spyropoulou-Stassinaki⁸², B.K. Srivastava⁸⁷, J. Stachel⁸⁶, I. Stan⁵³, I. Stan⁵³, G. Stefanek⁷³, M. Steinpreis¹⁸, E. Stenlund³¹, G. Steyn⁸³, J.H. Stiller⁸⁶, D. Stocco¹⁰⁵, M. Stolpovskiy⁴⁶, P. Strmen³⁵, A.A.P. Suade¹¹⁰, M.A. Subieta Vásquez²⁴, T. Sugitate⁴², C. Suire⁴⁵, R. Sultanov⁴⁹, M. Šumbera⁷⁷, T. Susa⁹⁰, T.J.M. Symons⁷⁰, A. Szanto de Toledo¹¹⁰, I. Szarka³⁵, A. Szczepankiewicz^{107,32}, A. Szostak¹⁷, M. Szymański¹²¹, J. Takahashi¹¹¹, J.D. Tapia Takaki⁴⁵, A. Tarantola Peloni⁵⁵, A. Tarazona Martinez³², A. Tauro³², G. Tejeda Muñoz¹, A. Telesca³², C. Terrevoli³⁰, J. Thäder⁸⁹, D. Thomas⁴⁸, R. Tieulent¹¹², A.R. Timmins¹¹³, D. Tlusty³⁶, A. Toia^{38,27,97}, H. Torii¹¹⁶, L. Toscano¹⁰¹, V. Trubnikov², D. Truesdale¹⁸, W.H. Trzaska⁴¹, T. Tsuji¹¹⁶, A. Tumkin⁹¹, R. Turrisi⁹⁷, T.S. Tveter²⁰, J. Ulery⁵⁵, K. Ullaland¹⁷, J. Ulrich^{64,54}, A. Uras¹¹², J. Urbán³⁷, G.M. Urciuoli⁹⁸, G.L. Usai²¹, M. Vajzer^{36,77}, M. Vala^{62,50}, L. Valencia Palomo⁴⁵, S. Vallero⁸⁶, P. Vande Vyvre³², M. van Leeuwen⁴⁸, L. Vannucci⁶⁹, A. Vargas¹, R. Varma⁴³, M. Vasileiou⁸², A. Vasiliev⁹², V. Vechernin¹²⁰, M. Veldhoen⁴⁸, M. Venaruzzo²³, E. Vercellin²⁴, S. Vergara¹, R. Vernet⁷, M. Verweij⁴⁸, L. Vickovic¹⁰⁶, G. Viesti²⁷, Z. Vilakazi⁸³, O. Villalobos Baillie⁹⁴, Y. Vinogradov⁹¹, L. Vinogradov¹²⁰, A. Vinogradov⁹², T. Virgili²⁸, Y.P. Viyogi¹¹⁹, A. Vodopyanov⁶², S. Voloshin¹²², K. Voloshin⁴⁹, G. Volpe³², B. von Haller³², D. Vranic⁸⁹, J. Vrláková³⁷, B. Vulpescu⁶⁶, A. Vyushin⁹¹, V. Wagner³⁶, B. Wagner¹⁷, R. Wan⁶, D. Wang⁶, Y. Wang⁸⁶, M. Wang⁶, Y. Wang⁶, K. Watanabe¹¹⁷, M. Weber¹¹³, J.P. Wessels^{32,57}, U. Westerhoff⁵⁷, J. Wiechula¹¹⁸, J. Wikne²⁰, M. Wilde⁵⁷, A. Wilk⁵⁷, G. Wilk⁷³, M.C.S. Williams¹⁰³, B. Windelband⁸⁶, L. Xaplanteris Karampatsos¹⁰⁸, C.G. Yaldo¹²², Y. Yamaguchi¹¹⁶, S. Yang¹⁷, H. Yang^{13,48}, S. Yasnopolskiy⁹², J. Yi⁸⁸, Z. Yin⁶, I.-K. Yoo⁸⁸, J. Yoon¹²⁶, W. Yu⁵⁵, X. Yuan⁶, I. Yushmanov⁹², V. Zaccolo⁷⁵, C. Zach³⁶, C. Zampolli¹⁰³, S. Zaporozhets⁶², A. Zarochentsev¹²⁰, P. Závada⁵², N. Zaviyalov⁹¹, H. Zbroszczyk¹²¹, P. Zelnicek⁵⁴, I.S. Zgura⁵³, M. Zhalov⁷⁹, H. Zhang⁶, X. Zhang^{66,6}, Y. Zhou⁴⁸, D. Zhou⁶, F. Zhou⁶, J. Zhu⁶, X. Zhu⁶, H. Zhu⁶, J. Zhu⁶, A. Zichichi^{22,11}, A. Zimmermann⁸⁶, G. Zinovjev², Y. Zoccarato¹¹², M. Zynov'yev², M. Zyzak⁵⁵

Affiliation notes

ⁱ Deceased

ⁱⁱ Also at: M.V.Lomonosov Moscow State University, D.V.Skobeltsyn Institute of Nuclear Physics, Moscow, Russia

ⁱⁱⁱ Also at: University of Belgrade, Faculty of Physics and "Vinča" Institute of Nuclear Sciences, Belgrade, Serbia

Collaboration Institutes

¹ Benemérita Universidad Autónoma de Puebla, Puebla, Mexico

² Bogolyubov Institute for Theoretical Physics, Kiev, Ukraine

³ Bose Institute, Department of Physics and Centre for Astroparticle Physics and Space Science (CAPSS), Kolkata, India

⁴ Budker Institute for Nuclear Physics, Novosibirsk, Russia

⁵ California Polytechnic State University, San Luis Obispo, California, United States

⁶ Central China Normal University, Wuhan, China

⁷ Centre de Calcul de l'IN2P3, Villeurbanne, France

⁸ Centro de Aplicaciones Tecnológicas y Desarrollo Nuclear (CEADEN), Havana, Cuba

⁹ Centro de Investigaciones Energéticas Medioambientales y Tecnológicas (CIEMAT), Madrid, Spain

- ¹⁰ Centro de Investigación y de Estudios Avanzados (CINVESTAV), Mexico City and Mérida, Mexico
¹¹ Centro Fermi – Centro Studi e Ricerche e Museo Storico della Fisica “Enrico Fermi”, Rome, Italy
¹² Chicago State University, Chicago, United States
¹³ Commissariat à l’Energie Atomique, IRFU, Saclay, France
¹⁴ COMSATS Institute of Information Technology (CIIT), Islamabad, Pakistan
¹⁵ Departamento de Física de Partículas and IGFAE, Universidad de Santiago de Compostela, Santiago de Compostela, Spain
¹⁶ Department of Physics Aligarh Muslim University, Aligarh, India
¹⁷ Department of Physics and Technology, University of Bergen, Bergen, Norway
¹⁸ Department of Physics, Ohio State University, Columbus, Ohio, United States
¹⁹ Department of Physics, Sejong University, Seoul, South Korea
²⁰ Department of Physics, University of Oslo, Oslo, Norway
²¹ Dipartimento di Fisica dell’Università and Sezione INFN, Cagliari, Italy
²² Dipartimento di Fisica dell’Università and Sezione INFN, Bologna, Italy
²³ Dipartimento di Fisica dell’Università and Sezione INFN, Trieste, Italy
²⁴ Dipartimento di Fisica dell’Università and Sezione INFN, Turin, Italy
²⁵ Dipartimento di Fisica dell’Università ‘La Sapienza’ and Sezione INFN, Rome, Italy
²⁶ Dipartimento di Fisica e Astronomia dell’Università and Sezione INFN, Catania, Italy
²⁷ Dipartimento di Fisica e Astronomia dell’Università and Sezione INFN, Padova, Italy
²⁸ Dipartimento di Fisica ‘E.R. Caianiello’ dell’Università and Gruppo Collegato INFN, Salerno, Italy
²⁹ Dipartimento di Scienze e Innovazione Tecnologica dell’Università del Piemonte Orientale and Gruppo Collegato INFN, Alessandria, Italy
³⁰ Dipartimento Interateneo di Fisica ‘M. Merlin’ and Sezione INFN, Bari, Italy
³¹ Division of Experimental High Energy Physics, University of Lund, Lund, Sweden
³² European Organization for Nuclear Research (CERN), Geneva, Switzerland
³³ Fachhochschule Köln, Köln, Germany
³⁴ Faculty of Engineering, Bergen University College, Bergen, Norway
³⁵ Faculty of Mathematics, Physics and Informatics, Comenius University, Bratislava, Slovakia
³⁶ Faculty of Nuclear Sciences and Physical Engineering, Czech Technical University in Prague, Prague, Czech Republic
³⁷ Faculty of Science, P.J. Šafárik University, Košice, Slovakia
³⁸ Frankfurt Institute for Advanced Studies, Johann Wolfgang Goethe-Universität Frankfurt, Frankfurt, Germany
³⁹ Gangneung-Wonju National University, Gangneung, South Korea
⁴⁰ Gauhati University, Department of Physics, Guwahati, India
⁴¹ Helsinki Institute of Physics (HIP) and University of Jyväskylä, Jyväskylä, Finland
⁴² Hiroshima University, Hiroshima, Japan
⁴³ Indian Institute of Technology Bombay (IIT), Mumbai, India
⁴⁴ Indian Institute of Technology Indore (IIT), Indore, India
⁴⁵ Institut de Physique Nucléaire d’Orsay (IPNO), Université Paris-Sud, CNRS-IN2P3, Orsay, France
⁴⁶ Institute for High Energy Physics, Protvino, Russia
⁴⁷ Institute for Nuclear Research, Academy of Sciences, Moscow, Russia
⁴⁸ Nikhef, National Institute for Subatomic Physics and Institute for Subatomic Physics of Utrecht University, Utrecht, Netherlands
⁴⁹ Institute for Theoretical and Experimental Physics, Moscow, Russia
⁵⁰ Institute of Experimental Physics, Slovak Academy of Sciences, Košice, Slovakia
⁵¹ Institute of Physics, Bhubaneswar, India
⁵² Institute of Physics, Academy of Sciences of the Czech Republic, Prague, Czech Republic
⁵³ Institute of Space Sciences (ISS), Bucharest, Romania
⁵⁴ Institut für Informatik, Johann Wolfgang Goethe-Universität Frankfurt, Frankfurt, Germany
⁵⁵ Institut für Kernphysik, Johann Wolfgang Goethe-Universität Frankfurt, Frankfurt, Germany
⁵⁶ Institut für Kernphysik, Technische Universität Darmstadt, Darmstadt, Germany
⁵⁷ Institut für Kernphysik, Westfälische Wilhelms-Universität Münster, Münster, Germany
⁵⁸ Instituto de Ciencias Nucleares, Universidad Nacional Autónoma de México, Mexico City, Mexico
⁵⁹ Instituto de Física, Universidad Nacional Autónoma de México, Mexico City, Mexico
⁶⁰ Institut of Theoretical Physics, University of Wroclaw

- 61 Institut Pluridisciplinaire Hubert Curien (IPHC), Université de Strasbourg, CNRS-IN2P3, Strasbourg, France
- 62 Joint Institute for Nuclear Research (JINR), Dubna, Russia
- 63 KFKI Research Institute for Particle and Nuclear Physics, Hungarian Academy of Sciences, Budapest, Hungary
- 64 Kirchhoff-Institut für Physik, Ruprecht-Karls-Universität Heidelberg, Heidelberg, Germany
- 65 Korea Institute of Science and Technology Information, Daejeon, South Korea
- 66 Laboratoire de Physique Corpusculaire (LPC), Clermont Université, Université Blaise Pascal, CNRS-IN2P3, Clermont-Ferrand, France
- 67 Laboratoire de Physique Subatomique et de Cosmologie (LPSC), Université Joseph Fourier, CNRS-IN2P3, Institut Polytechnique de Grenoble, Grenoble, France
- 68 Laboratori Nazionali di Frascati, INFN, Frascati, Italy
- 69 Laboratori Nazionali di Legnaro, INFN, Legnaro, Italy
- 70 Lawrence Berkeley National Laboratory, Berkeley, California, United States
- 71 Lawrence Livermore National Laboratory, Livermore, California, United States
- 72 Moscow Engineering Physics Institute, Moscow, Russia
- 73 National Centre for Nuclear Studies, Warsaw, Poland
- 74 National Institute for Physics and Nuclear Engineering, Bucharest, Romania
- 75 Niels Bohr Institute, University of Copenhagen, Copenhagen, Denmark
- 76 Nikhef, National Institute for Subatomic Physics, Amsterdam, Netherlands
- 77 Nuclear Physics Institute, Academy of Sciences of the Czech Republic, Řež u Prahy, Czech Republic
- 78 Oak Ridge National Laboratory, Oak Ridge, Tennessee, United States
- 79 Petersburg Nuclear Physics Institute, Gatchina, Russia
- 80 Physics Department, Creighton University, Omaha, Nebraska, United States
- 81 Physics Department, Panjab University, Chandigarh, India
- 82 Physics Department, University of Athens, Athens, Greece
- 83 Physics Department, University of Cape Town and iThemba LABS, National Research Foundation, Somerset West, South Africa
- 84 Physics Department, University of Jammu, Jammu, India
- 85 Physics Department, University of Rajasthan, Jaipur, India
- 86 Physikalisches Institut, Ruprecht-Karls-Universität Heidelberg, Heidelberg, Germany
- 87 Purdue University, West Lafayette, Indiana, United States
- 88 Pusan National University, Pusan, South Korea
- 89 Research Division and ExtreMe Matter Institute EMMI, GSI Helmholtzzentrum für Schwerionenforschung, Darmstadt, Germany
- 90 Rudjer Bošković Institute, Zagreb, Croatia
- 91 Russian Federal Nuclear Center (VNIIEF), Sarov, Russia
- 92 Russian Research Centre Kurchatov Institute, Moscow, Russia
- 93 Saha Institute of Nuclear Physics, Kolkata, India
- 94 School of Physics and Astronomy, University of Birmingham, Birmingham, United Kingdom
- 95 Sección Física, Departamento de Ciencias, Pontificia Universidad Católica del Perú, Lima, Peru
- 96 Sezione INFN, Bari, Italy
- 97 Sezione INFN, Padova, Italy
- 98 Sezione INFN, Rome, Italy
- 99 Sezione INFN, Catania, Italy
- 100 Sezione INFN, Cagliari, Italy
- 101 Sezione INFN, Turin, Italy
- 102 Sezione INFN, Trieste, Italy
- 103 Sezione INFN, Bologna, Italy
- 104 Nuclear Physics Group, STFC Daresbury Laboratory, Daresbury, United Kingdom
- 105 SUBATECH, Ecole des Mines de Nantes, Université de Nantes, CNRS-IN2P3, Nantes, France
- 106 Technical University of Split FESB, Split, Croatia
- 107 The Henryk Niewodniczanski Institute of Nuclear Physics, Polish Academy of Sciences, Cracow, Poland
- 108 The University of Texas at Austin, Physics Department, Austin, TX, United States
- 109 Universidad Autónoma de Sinaloa, Culiacán, Mexico
- 110 Universidade de São Paulo (USP), São Paulo, Brazil

- ¹¹¹ Universidade Estadual de Campinas (UNICAMP), Campinas, Brazil
¹¹² Université de Lyon, Université Lyon 1, CNRS/IN2P3, IPN-Lyon, Villeurbanne, France
¹¹³ University of Houston, Houston, Texas, United States
¹¹⁴ University of Technology and Austrian Academy of Sciences, Vienna, Austria
¹¹⁵ University of Tennessee, Knoxville, Tennessee, United States
¹¹⁶ University of Tokyo, Tokyo, Japan
¹¹⁷ University of Tsukuba, Tsukuba, Japan
¹¹⁸ Eberhard Karls Universität Tübingen, Tübingen, Germany
¹¹⁹ Variable Energy Cyclotron Centre, Kolkata, India
¹²⁰ V. Fock Institute for Physics, St. Petersburg State University, St. Petersburg, Russia
¹²¹ Warsaw University of Technology, Warsaw, Poland
¹²² Wayne State University, Detroit, Michigan, United States
¹²³ Yale University, New Haven, Connecticut, United States
¹²⁴ Yerevan Physics Institute, Yerevan, Armenia
¹²⁵ Yildiz Technical University, Istanbul, Turkey
¹²⁶ Yonsei University, Seoul, South Korea
¹²⁷ Zentrum für Technologietransfer und Telekommunikation (ZTT), Fachhochschule Worms, Worms, Germany